Hindawi
Geofluids
Volume 2020, Article ID 6418215, 12 pages
https://doi.org/10.1155/2020/6418215

Research Article

The Estimation of Reservoir Temperature for Thermal Springs Using the Integrated Multicomponent Geothermometry Method at Changbai Mountain, Northeastern Songliao Basin, China

Jin Na,[1] Bai-zhong Yan,[2,3] Bao-ming Chi,[4] Bo Feng,[5] and Xue Jiang[6]

[1]*College of Resources and Environment, Yangtze University, 430100 Wuhan, Hubei, China*
[2]*School of Water Resources & Environment, Hebei GEO University, Shijiazhuang 050031, China*
[3]*Engineering Research Center of Geothermal Resources Development Technology and Equipment, Ministry of Education, Jilin University, Changchun 130026, China*
[4]*Institute of Disaster Prevention, Sanhe 065201, China*
[5]*Key Lab of Groundwater Resources and Environment, Ministry of Education/College of New Energy and Environment, Jilin University, Changchun 130021, China*
[6]*School of Environmental Studies, China University of Geosciences, Wuhan 430074, China*

Correspondence should be addressed to Bai-zhong Yan; jluybz@126.com, Bao-ming Chi; chibaoming@126.com, and Xue Jiang; jiangxue100@163.com

Received 21 June 2019; Revised 30 September 2019; Accepted 5 November 2019; Published 18 January 2020

Academic Editor: Carmine Apollaro

The Changbai Mountain volcanic region, eastern Songliao Plain, China, is considered a potential target development area for geothermal water exploitation. To assess the feasibility of geothermal development, we applied integrated multicomponent geothermometry (IMG) in the program GeoT to estimate the geothermal reservoir temperatures for four major thermal springs in this area. Numerical optimizations of Al and HCO_3^- concentrations, dilutions, and steam fractions were conducted to reconstruct the original deep fluid compositions by the IMG method. The results show that the geothermal reservoir temperatures of these springs range from 118 to 172°C in the Changbai Mountain volcanic region. In contrast to classic geothermometers, the IMG method can quantify processes affecting the fluid chemical composition and yield reasonable temperatures. The reservoir temperatures for the Julong and Jinjiang thermal springs are significantly greater than those for the Shibadaogou and Xianrenqiao thermal springs. Moreover, the geothermal deep circulation characteristics of the above springs are also investigated based on reservoir temperature estimates. The methods presented in this study could be applied to other geothermal fields under similar geothermal resource conditions.

1. Introduction

China has demonstrated the feasibility of improving the local economy and reducing carbon emissions through geothermal energy development. Changbai Mountain in the eastern Songliao Plain, China, displays widespread geothermal activity indicating that it is abnormally hot. Julong springs, Jinjiang springs, Shibadaogou springs, and Xianrenqiao springs are major thermal springs in the Changbai Mountain area. In recent years, an action plan for use of geothermal water has been launched in the region with negative assenting reservoir temperature, which is difficult to measure directly. However, the temperatures of geothermal reservoir fluids in the Changbai Mountain volcanic region are not clear.

In recent decades, chemical geothermometers have been used to evaluate geothermal reservoir temperature by analysing the relationship between deep fluid chemical composition and reservoir temperature. The fluid samples in the

analysis could be collected at the ground surface from exploration wells and hot springs. These classic geothermometers have been successfully applied to many geothermal waters (Spycher et al., 2012), such as the Na-K [1, 2], Na-K-Ca [3], silica [4], and K-Mg geothermometers [2]. The silica geothermometer is based on the solubility of silica minerals and is generally used in geothermal reservoirs above 150°C. The Na-K geothermometer is based on the equilibrium between alkali feldspar and geothermal reservoir fluids and is generally assumed to apply in deep reservoir temperature estimation. The Na-K-Ca geothermometer is usually regarded as a revision of the Na-K geothermometer for application to Ca-rich waters of geothermal reservoirs. Based on the equilibrium of geothermal fluids with clinochlore, muscovite, and K-feldspar, the K-Mg geothermometer is generally considered to reflect shallow geothermal reservoir temperatures. All the classic geothermometers apply to chemical equilibrium (or near-equilibrium) between geothermal reservoir fluid and reservoir minerals. However, the dilution, boiling, and gas escape processes that occur when deep reservoir fluid ascends to the ground surface can mask deep geochemical signatures (Spycher et al., 2014). Yan et al. [5] investigated the conceptual genetic model of thermal springs in the Changbai Mountain region and suggested that the deep thermal fluid may be mixed with shallow cool water and react with minerals as it moves upward.

The integrated multicomponent geothermometry (IMG) approach presented by Reed and Spycher [6] presents advantages over classic geothermometers, and it has been formulated into a computer program (GeoT). According to the theoretical thermodynamic chemical equilibration of multiple minerals with geothermal reservoir fluid, this program can reconstruct the chemical composition in deep fluids and then automatically estimate reservoir temperatures. Compared with classic geothermometers, IMG corrects chemical reactions, dilution, and boiling affecting the fluid chemical composition as it ascends from depth to the ground surface. The method has been validated in context using fluid analyses, numerical simulations, and mineralogical data from geothermal systems [7, 8].

The main objective of this study is to calculate an accurate reservoir temperature for thermal springs in the Changbai Mountain volcanic region. IMG is first applied to reconstruct the original deep fluid compositions from chemical or physical processes in the genesis of thermal springs and to assess geothermal reservoir conditions in this study area. The results of this study could promote geothermal development in the Changbai Mountain volcanic region.

2. Geological and Hydrogeological Setting

The Changbai Mountain volcanic region is located in Northeast China and has active volcanoes (Figure 1). The elevation in this region ranges from 700 to 3000 m. This area has a temperate continental monsoon climate with an annual average temperature of 3.5°C, and its average precipitation is 1332.6 mm. The basement in the region is composed of Archean and Proterozoic metamorphic rocks. The stratigraphic sequence of deposits from the Cenozoic to the Proterozoic age is commonly divided into more than 30 members. The Mesozoic sediments are overlain by rhyolite and an expansive Cenozoic basalt platform capped by the Tianchi volcano, a famous active volcano in the centre of the volcanic region. The region has experienced multistage tectonic activity that has resulted in faults that act as ascent pathways for deep reservoir fluids. The volcanic activity can be categorized into four main stages from Miocene to Holocene [9, 10], and it is closely related to widespread geothermal activity in the Changbai Mountain volcanic region.

The origins of the four major groups of thermal springs in our study area (Figure 1) have been studied by Yan et al. [5]. Julong and Jinjiang springs lie near the Tianchi volcano crater and derive heat from its magma chamber. Xianrenqiao springs and Shibadaogou springs are 40 km and 80 km distant from the Tianchi volcano crater. Yan et al. [5] suggested that the geothermal reservoir of Julong and Jinjiang thermal springs is a fracture zone in the volcanic rocks and marble in the Proterozoic Laoling Formation. The geothermal reservoir of Shibadaogou thermal springs is a fracture zone in the Cambrian-Sinian limestone and sandstone, and the Xianrenqiao thermal reservoir is a fracture zone in the Ordovician-Cambrian limestone and sandstone [5]. The porosity and permeability of thermal reservoir were 3%~6% and $1 \times 10^{-3}\mu m^2 \sim 10 \times 10^{-3}\mu m^2$ [11]. The schematic geological section [5] showed that the hot spring water is mainly supplied by precipitation when expelled on the surface along the fault zones by deep circulation. The heat source for the Julong and Jinjiang thermal springs is conduction from the magma under the Tianchi volcano; that for the Shibadaogou and Xianrenqiao thermal springs is radioactive decay heat from Jurassic granite [12].

3. Hydrogeochemical Characteristics of Thermal Springs

The geochemical data (Table 1) for thermal springs in this study originate from the analyses of spring waters by Yan [12]. The maximum temperature of Julong is 84°C and the Jinjiang maximum is 58°C while those of the Shibadaogou and Xianrenqiao thermal springs are 35°C and 44°C, respectively. The pH values for the Julong and Jinjiang thermal springs range from 6.65 to 7.34, while those of the Shibadaogou and Xianrenqiao thermal springs range from 7.03 to 7.8. A Piper diagram (Figure 2) shows that the springs are dominated by Na^+ and HCO_3^-. Comparing with cold ground water (Table 1), thermal spring water has significantly higher concentrations of major ions due to water-rock interaction.

The relationship between Cl^- and Na^+ concentrations (Figure 3(a)) is usually used to reveal a dilution process as the deep reservoir fluid ascends to the surface [8]. The specified deviations of Na/Cl trends in the Julong-Jinjiang thermal springs and Shibadaogou-Xianrenqiao thermal springs are shown in Figure 3(a), as they originate from different deep heat reservoirs and then draw on different hydrothermal systems. Figure 3(b) shows general positive correlations between Si concentration and spring temperature in the Julong and Shibadaogou springs, probably because dissolution of silicate minerals increases with the temperature

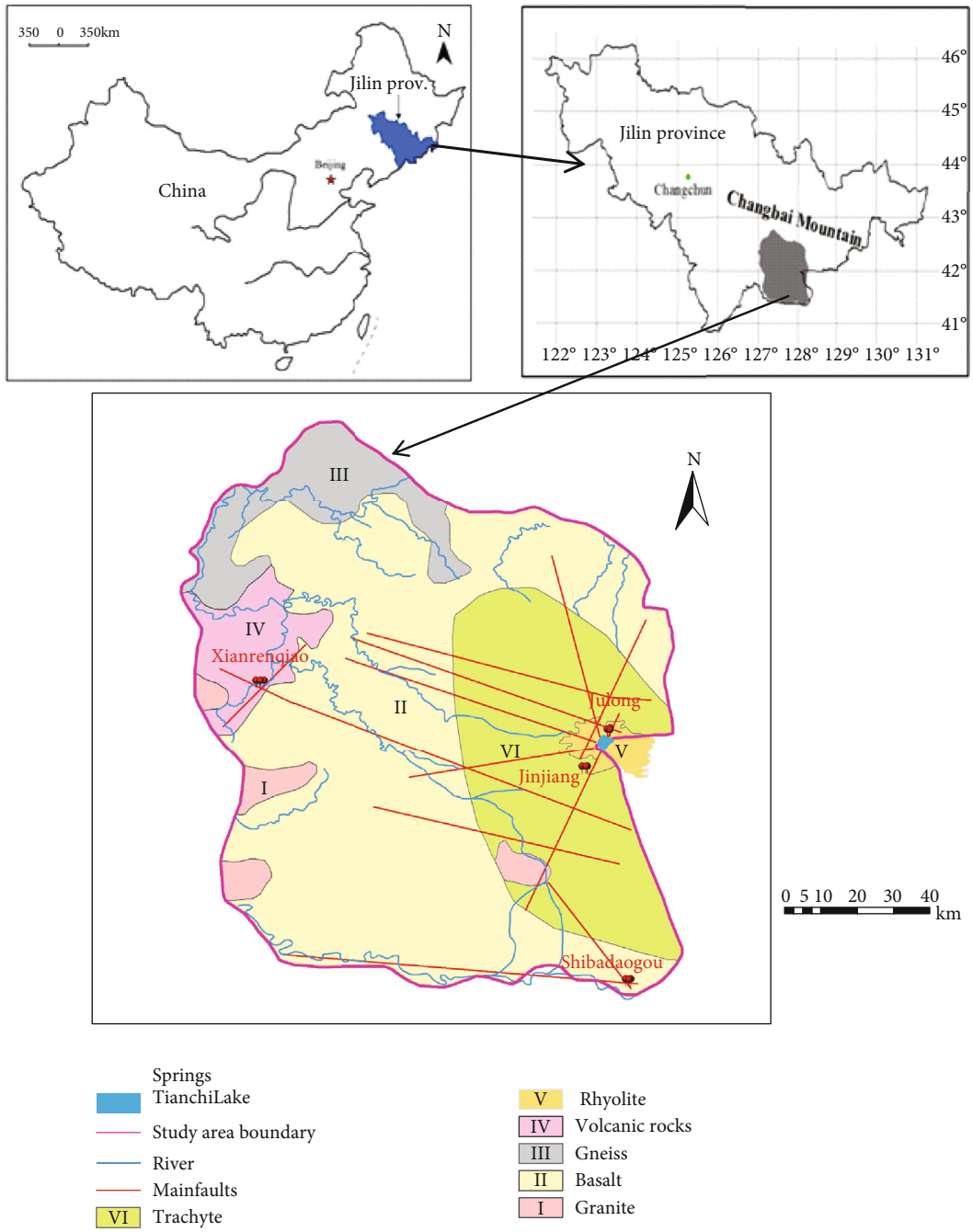

Figure 1: Geology and hydrogeology in the Changbai Mountain region [5, 13].

and circulation path of the geothermal fluid [14]. The concentrations of K and Na are generally correlated with Si (Figures 3(c) and 3(d)) in thermal springs. This relation could be explained by their origin from the dissolution of albite and K-feldspar in the reservoir.

4. Integrated Multicomponent Geothermometry Approach

4.1. Simulation Program. The computer program for multicomponent geothermometry (GeoT) is applied in this study [15–17]. The existing routines and methods, including TOUGHREACT [18–20], SOLVEQ/CHILLER [21, 22], and GEOCAL [6], were utilized in GeoT. According to the chemical analyses of spring samples, GeoT computes the saturation indices (log (Q/K)) of minerals in a thermal reservoir through a range of reservoir temperatures from 25 to 300°C using the thermodynamic equilibrium constant (K) from a thermodynamic database and the activity coefficients and mineral ion activity product (Q) computed for each water analysis. Then, the clustering of log (Q/K) curves near zero at any specific temperature for certain reservoir minerals is an indication of the reservoir temperature. GeoT also allows numerical optimization of inaccurate and unknown input

Table 1: Hydrogeochemical data of selected thermal water samples from the Changbai Mountain volcanic region (mg/L).

Sample no.	Water sample types	T (°C)	pH	K^+	Na^+	Ca^{2+}	Mg^{2+}	Cl^-	SO_4^{2-}	HCO_3^-	Si	TDS	Hydrochemical type
G01	Julong springs	84	7.34	19.42	347.40	37.20	3.22	114.43	—	903.02	76.08	1471.79	HCO_3-Na
G02		82	7.12	20.02	363.15	37.20	4.30	104.89	—	897.21	77.33	1596.75	HCO_3-Na
G03	Jinjiang springs	36	6.65	13.48	168.70	31.89	19.33	30.67	16.98	603.95	49.06	1000.13	HCO_3-Na
G04		45	7.05	21.94	284.30	30.12	11.81	53.50	21.23	827.53	56.43	1034.88	HCO_3-Na
G05		55	6.76	19.56	235.10	30.12	16.11	47.79	—	752.03	64.22	1246.94	HCO_3-Na
G06		58	6.65	25.62	285.95	33.66	13.94	59.12	21.23	871.08	83.38	1506.38	HCO_3-Na
G07	Shibadaogou springs	35.5	7.04	10.82	324.40	31.89	6.44	123.97	84.92	702.67	24.468	1344.8	HCO_3-Na
G08		35	7.03	10.61	308.10	35.43	13.96	123.97	84.92	720.09	23.52	1354.38	HCO_3-Na
G09		35	7.34	10.81	328.70	30.12	19.33	133.50	106.15	711.38	24.67	1400.10	HCO_3-Na
G10	Xianrenqiao springs	44	7.80	9.94	326.10	31.89	13.96	133.50	297.22	371.66	32.30	1261.56	HCO_3·SO_4-Na
G11	Cold ground water	9	6.96	1.22	3.10	8.86	4.30	2.85	8.49	46.46	11.64	100.50	HCO_3-Ca·Mg

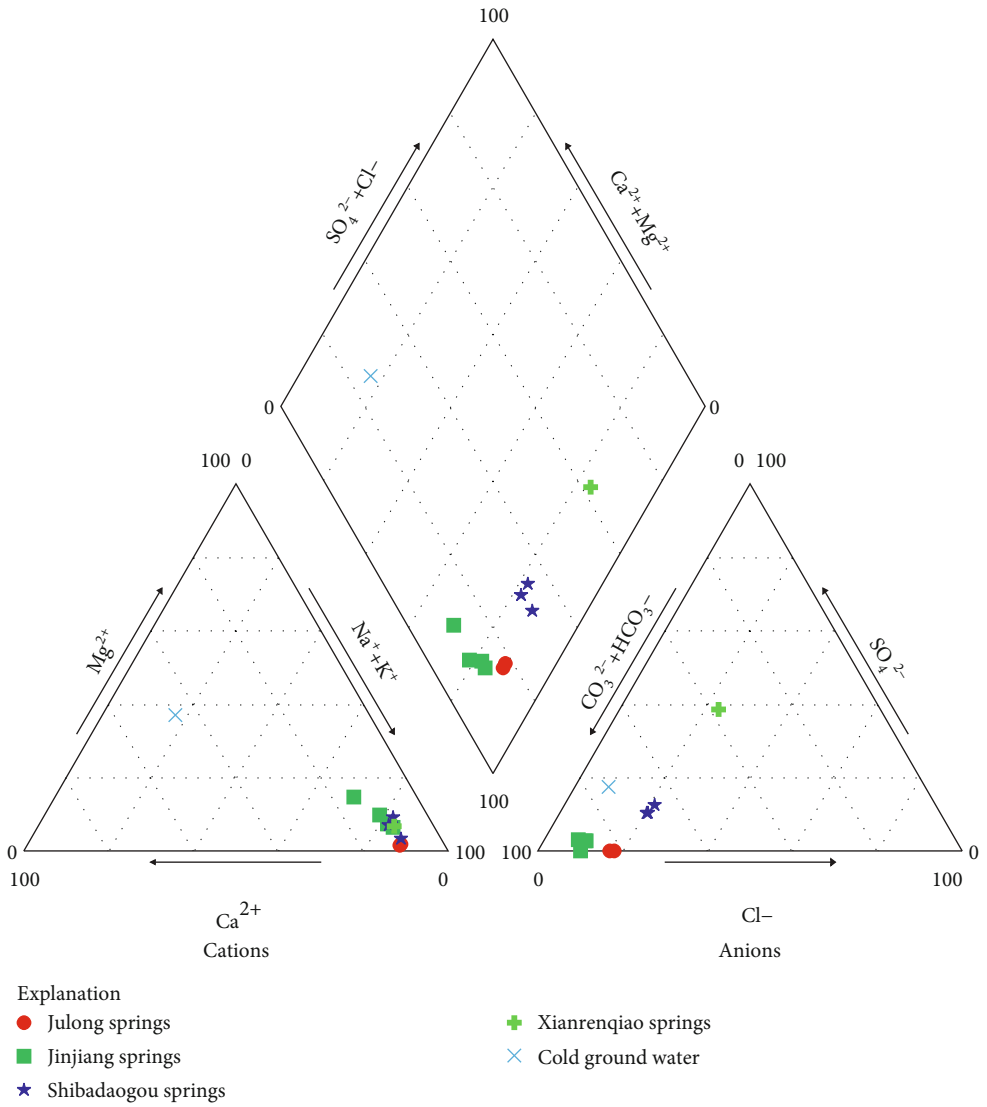

Figure 2: Piper diagram for thermal spring water samples from the Changbai Mountain volcanic region.

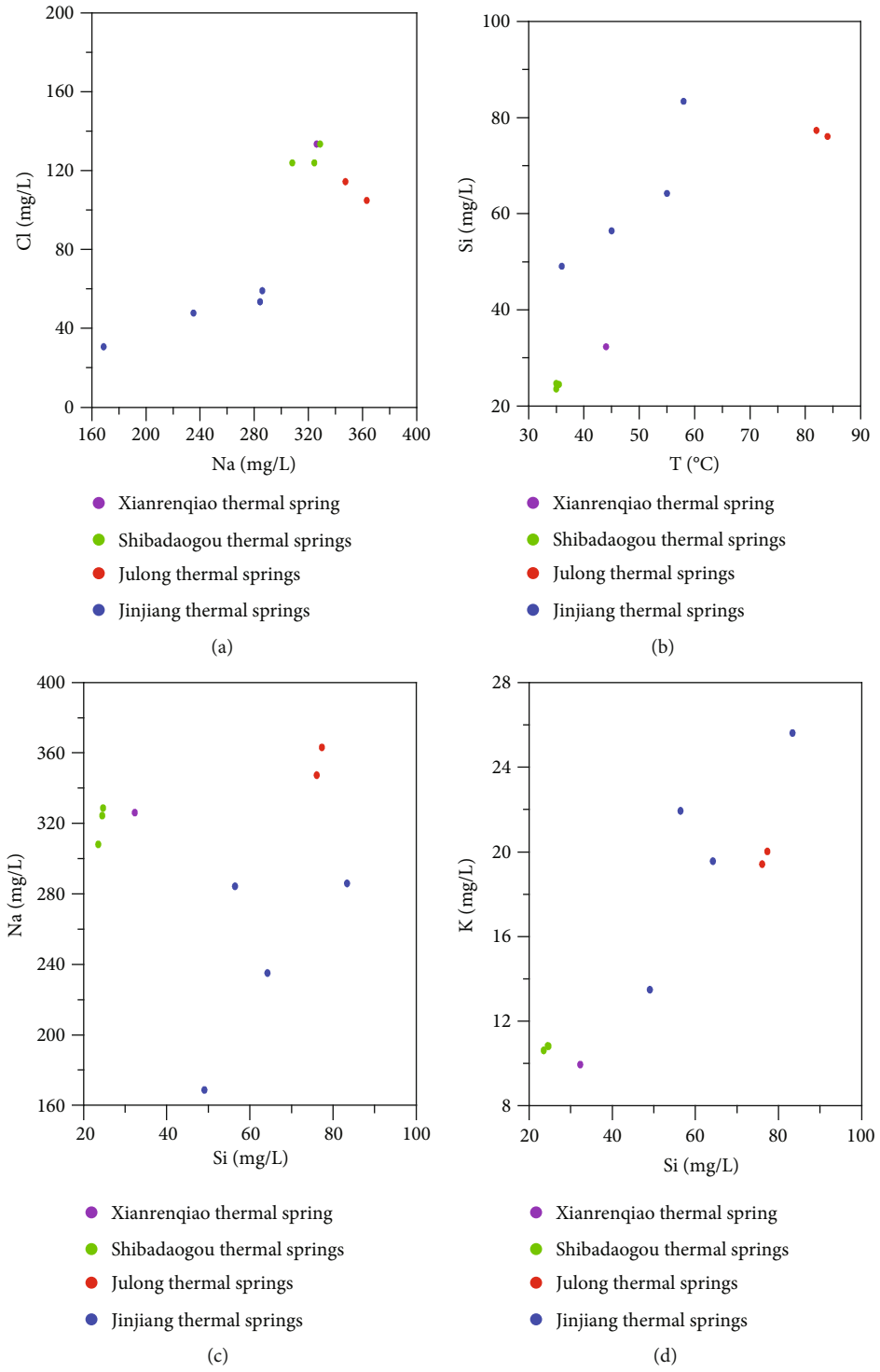

Figure 3: (a) Na vs. Cl concentration plot for thermal spring samples. (b) Si-temperature relationships for thermal spring samples. (c) Na vs. Si concentration plot for thermal spring samples. (d) K vs. Si concentration plot for thermal spring samples.

parameters (e.g., dilution/mixing and gas loss) affecting temperature estimates that rely on deep fluid reconstruction. The geothermometry simulation estimates reservoir temperatures by combining fluid reconstruction and numerical optimization in GeoT called the IMG method. This approach has been successfully applied to many geothermal systems [23–26]. For the details, refer to Spycher et al. (2014).

4.2. Thermodynamic Data and Mineral Assemblage. The thermodynamic database applied in our study is SOLTHERM, which has been successfully used to simulate various types of geothermal fluid systems [21, 27–29].

A mineral assemblage in the log (Q/K) results is adopted based on the literature [12], which shows that the geothermal reservoir of the Julong and Jinjiang hot springs is volcanic

rocks and marble with significant silicification, while for the Shibadaogou-Xianrenqiao thermal springs, it is sandstone and limestone. According to Wang [30] and Lian [31], the Julong and Jinjiang hot spring reservoir contains calcite, quartz, actinolite, albite, microcline, tremolite, dolomite, ankerite, and amorphous silica, and kaolinite, illite, calcite, quartz, albite, microcline, montmorillonite-Na, dolomite, and montmorillonite-Ca appear in the Shibadaogou-Xianrenqiao thermal spring reservoir.

5. Results and Discussion

5.1. Insights from a Single Spring. G01 (Julong hot spring) is closest to the volcano crater and has a relatively high temperature (84°C); an initial analysis of the sample is conducted. In the base case, the cross average temperature is calculated to be 122°C by evaluating the saturation indices of all 9 minerals in the reservoir (Figure 4(a)). Notably, the obtained mineral saturation indices (SI) reveal poor clustering as a function of temperature without deep fluid reconstruction. Therefore, deep fluid construction should be accomplished by the IMG method to estimate the reservoir temperature.

The numerical optimization of deep fluid construction is achieved with the combination of trial and error and external numerical optimization software (PEST). The concentrations of Al and HCO_3^- are low-accuracy input parameters in GeoT, as the Al concentration is usually lower than the detection limit and the aqueous HCO_3^- in the spring sample can be diminished by decarbonation when deep geothermal fluid moves up to the surface, strongly affecting reservoir temperature estimation. Following the "Fix-Al" method proposed by Pang and Reed [27], the Al concentration of the deep fluid can be optionally corrected by the assumption that its concentration is forced by thermodynamic equilibrium with an Al-containing mineral. The approach has been effective for geothermal reservoirs with Al-containing minerals (Pang and Reed; 2010). In this study, there are two Al-containing minerals (albite and microcline) in the Julong hot spring reservoir, and the aqueous Al is forced to yield equilibrium with microcline. Moreover, the main carbonate minerals in the thermal reservoir are calcite and dolomite. Considering that the Ca^{2+} concentration is significantly greater than the Mg^{2+} concentration in the water sample, the HCO_3^- concentration is constrained by forcing equilibrium with calcite [28]. In the application of the optional calculation for aqueous Al and HCO_3^-, the log (Q/K) curves of Al-containing minerals and carbonate minerals show relatively good clustering, and a temperature of 187°C is obtained in GeoT based on the 7 best clustering minerals in Figure 4(b). However, the clustering of saturation index curves for other minerals is relatively poor. Moreover, there are four types of statistical analyses in the GeoT program, which helps us conduct the temperature estimation and judge the clustering of mineral curves accurately. The minimum of median analysis (RMED) is usually used for the final temperature estimation, and other statistical analyses (RMSE: root mean square error; SDEV: standard deviation; mean: average) are applied to identify the quality of the clustering [15]. In GeoT, the clustering is considered good on the condition that the minimum of the log (Q/K) statistics is less than 0.1. The minimum of RMED and other statistical analyses depart significantly from zero in Figure 4(c). Therefore, the above reservoir temperature estimation with deep fluid reconstruction through the Fix-Al-HCO_3^- method in numerical optimization shows a large uncertainty.

In addition to the use of the Fix-Al-HCO_3^- method, the numerical optimizations of the dilution factor and the steam fraction are applied here to reconstruct the deep fluid compositions by minimizing the clustering of mineral saturation indices. In GeoT, the dilution factor is used to represent the dilution effect when its value is greater than 1. The steam fraction represents the gas content in the total discharge and is used to add the steam loss by boiling into the solution. The main dry gas composition in gas samples of the Julong hot spring is 96 mol% CO_2 and 4 mol% N_2. Considering that the major "dry" gas of the Julong spring is CO_2, the steam fraction is used to calibrate for the CO_2 loss effect on the chemical equilibrium of the deep fluid with reservoir minerals. After the numerical optimization for these parameters in geothermal water reconstruction, $T_{RMED} = 167°C$ is obtained based on the 7 best clustering minerals, while ankerite remains supersaturated in the deep fluid in the reservoir (Figures 4(d) and 4(e)). The minimum of RMED in this case is 0.03 (Figure 4(f)), and the spread of the calculated temperature results is less than 20°C, showing that this value is better constrained than the previous temperature estimate. The steam fraction is 0.23, representing significant steam loss in the Julong hot spring. The dilution/concentration factor is 1.17, which means that the water compositions are corrected based on the dilution effect in the mixing process of the deep fluid with shallow groundwater.

5.2. Reservoir Temperature Estimations. In addition to the thermal spring G01, we used the above IMG method to investigate the reservoir temperature for other thermal springs in the Changbai Mountain volcanic region. The dry gas composition in samples of the Jinjiang hot spring is 79 mol% CO_2 and 21 mol% N_2, and in the Shibadaogou and Xianrenqiao geothermal spring samples, it is 6 mol% CO_2 and 94 mol% N_2 [12]. All of the results estimated by IMG with the justification for each sample are listed in Table 2, and the calculated mineral saturation indices (SI) are relatively good (Figure 5).

Julong hot springs yield estimated reservoir temperatures of 167°C and 172°C, and Jinjiang springs yield 170°C, 156°C, and 162°C (Figure 6). Estimated reservoir temperatures between 110 and 130°C were obtained for samples from the Shibadaogou and Xianrenqiao springs. These data indicate that the temperatures in the Julong and Jinjiang springs are significantly higher than those in the Shibadaogou and Xianrenqiao springs, as estimated by IMG. Their deep meteoric fluid is heated by a magma chamber, resulting in a high-temperature reservoir. The Shibadaogou and Xianrenqiao springs are far from the volcanic crater, and their geothermal condition results from deep crustal fractures.

Estimated reservoir temperatures based on quartz and chalcedony geothermometers [5] are compared with the estimated temperatures by IMG in Figure 6 and Table 2.

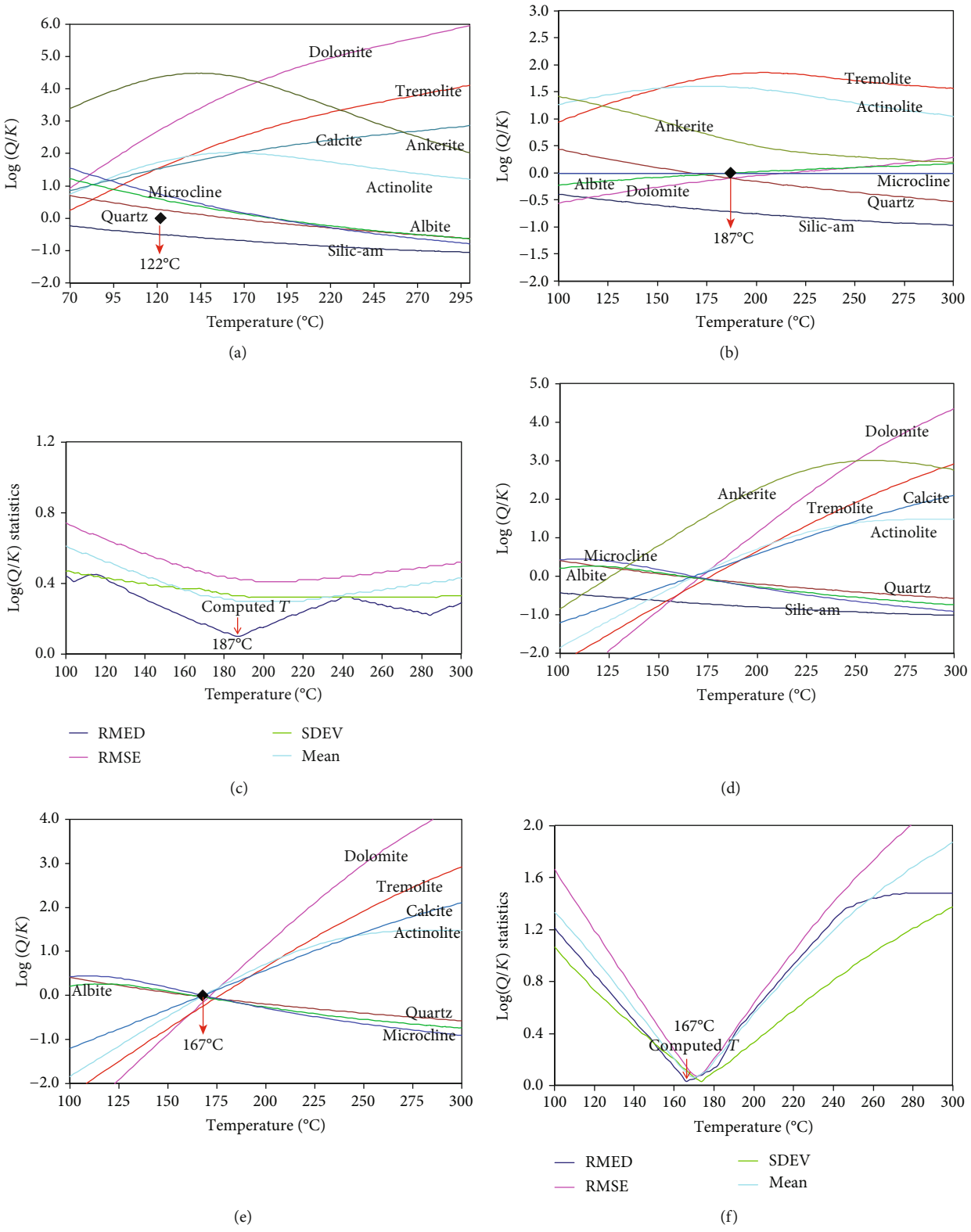

FIGURE 4: Simulation results for water sample G01 in the Julong thermal spring obtained by the integrated multicomponent geothermometry method. (a) Mineral saturation index variation with temperature for the base case. (b) Mineral saturation index variation with temperature for the Fix-Al-HCO_3^- case. (c) Statistical analysis for the Fix-Al-HCO_3^- case. (d) Mineral saturation index variation with temperature for the water-reconstructed case, considering all the minerals. (e) Mineral saturation index variation with temperature for the water-reconstructed case, considering the main minerals. (f) Statistical analysis for the water-reconstructed case (considering the major minerals).

Table 2: Temperature estimates by classic geothermometers and IMG and values of the optimization parameters for deep fluid construction.

Sample no.	Thermal springs	$T_{measured}$ (°C)	Original fluid (°C) [12]		Reconstructed fluid (°C)					T_{GeoT} (°C)	Optimized parameters		Equilibrium mineral assemblages
			T_{quartz}	$T_{chalcedony}$	$T_{chalcedony}$	T_{quartz}	T_{Na-K}	$T_{Na-K-Ca}$	T_{K-Mg}		sf	cfact	
G01	Julong hot springs I	84	163	157	136	160	190	157	95	167	0.23	1.17	Calcite, quartz, albite, microcline, tremolite, actinolite, and dolomite
G02	Julong hot springs II	82	166	156	142	166	189	157	93	172	0.13	1.11	Calcite, quartz, albite, microcline, tremolite, and dolomite
G03	Jinjiang hot springs I	36	138	114	142	166	215	168	70	170	0.24	2.0	Calcite, quartz, albite, microcline, tremolite, and actinolite
G04	Jinjiang hot springs II	45	121	142	121	147	212	172	83	153	0.2	1.22	Calcite, quartz, albite, microcline, tremolite, actinolite, and dolomite
G05	Jinjiang hot springs III	55	138	148	122	147	218	172	74	162	0.29	1.22	Calcite, quartz, albite, microcline, tremolite, and actinolite
G06	Jinjiang hot springs IV	58	179	162	140	164	224	178	83	162	0.29	1.22	Calcite, quartz, albite, microcline, tremolite, and actinolite
G07	Shibadaogou hot springs I	35.5	104	74	102	130	158	137	79	130	0.00	1.66	Calcite, dolomite, albite, quartz, microcline, and montmorillonite-Na
G08	Shibadaogou hot springs II	35	102	72	103	131	159	138	70	110	0.00	1.76	Calcite, quartz, albite, microcline, and dolomite
G09	Shibadaogou hot springs III	35	104	75	102	130	157	137	66	118	0.03	1.70	Calcite, quartz, albite, microcline, montmorillonite-Na, and montmorillonite-Ca
G10	Xianrenqiao hot spring	44	118	89	109	136	152	132	66	127	0.00	1.40	Calcite, quartz, albite, microcline, montmorillonite-Na, dolomite, and kaolinite

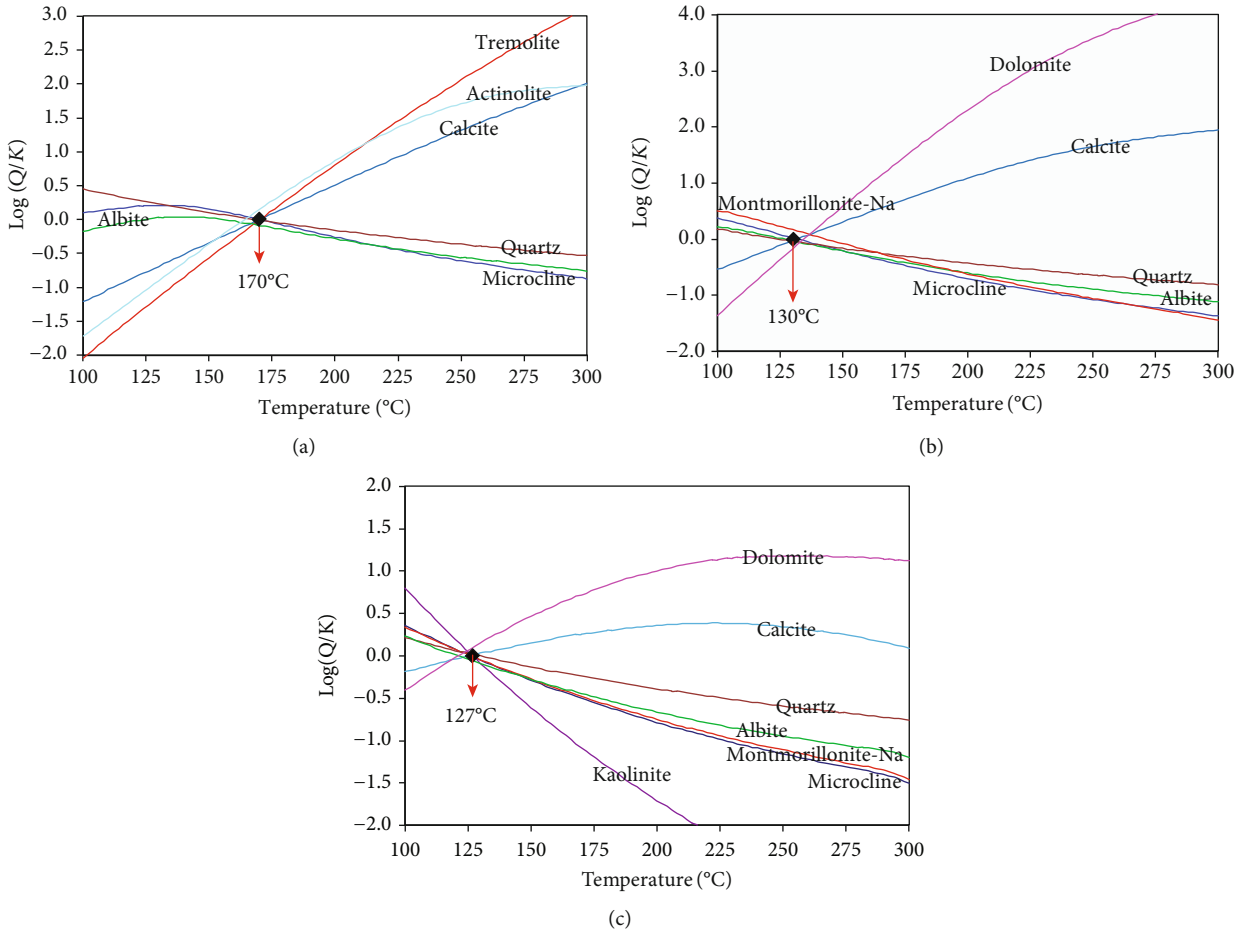

Figure 5: Mineral saturation index variation with temperature for (a) G03 water sample in Jinjiang springs, (b) G07 water sample in Shibadaogou springs, and (c) G10 water sample in Xianrenqiao springs.

Chemical reaction, dilution, and boiling of spring waters produce differences between the classic geothermometer results and IMG temperature estimates. The results of the quartz and Na-K-Ca geothermometers after IMG deep fluid reconstruction are generally closest to the temperatures estimated by IMG (Figures 6 and 7) while other classic geothermometers yield hardly reasonable results. It then appears that deep fluid reconstruction in the reservoir temperature estimation is unlikely to obtain good results for all classic geothermometers, but it could correct the clustering of calculated mineral SI curves (Hou et al., 2017). Yan et al. [5] showed the results of the Ca-K-Na Giggenbach plot with the thermal spring water sample plot in an immature field, possibly due to mixing with surface groundwater, which indicated that the classic Na-K-Ca geothermometer is not favorable for estimating geothermal reservoir temperatures in the Changbai Mountain region.

The steam fractions (sf) for the Julong and Jinjiang springs in the numerical optimization (Table 2) range from 0.13 to 0.29, indicating spring samples affected by steam loss. Moreover, there are CO_2-rich gases emerging from the Julong and Jinjiang springs, which support this finding of gas loss. The Julong and Jinjiang springs are located in volcanically active and fault areas. The steam fractions obtained in Shibadaogou and Xianrenqiao springs are much smaller than those in the Julong and Jinjiang springs, which is consistent with an absence of significant degassing at the Shibadaogou and Xianrenqiao springs in the field reconnaissance. In numerical optimization, the computed dilution factors (cfact, Table 2) reflect shallower mixing processes. In these springs, all of the factors used for geothermal water construction are higher than "1.0" to correct the mixing between the deep fluid and shallow water by the IMG method. Considering the generally similar reservoir temperature estimates and steam fractions in the Julong and Jinjiang springs, it is likely that these water samples share a common deep geothermal reservoir. As shown in Table 2, the dilution factors in the Shibadaogou and Xianrenqiao springs are significantly greater than those in the Julong and Jinjiang springs, except for sample G03 of Jinjiang springs, revealing a closer hydraulic relation between the shallow and deep geothermal reservoirs. Yan et al. [5] investigated the mixing process with shallow groundwater in these springs by a Na-K-Ca Giggenbach plot, which also indicated more shallow water in the Shibadaogou and Xianrenqiao springs than in the Julong and Jinjiang springs.

5.3. Geothermal Deep Circulation Characteristics. The geothermal deep circulation characteristics were investigated based on reservoir temperature using the IMG method. The

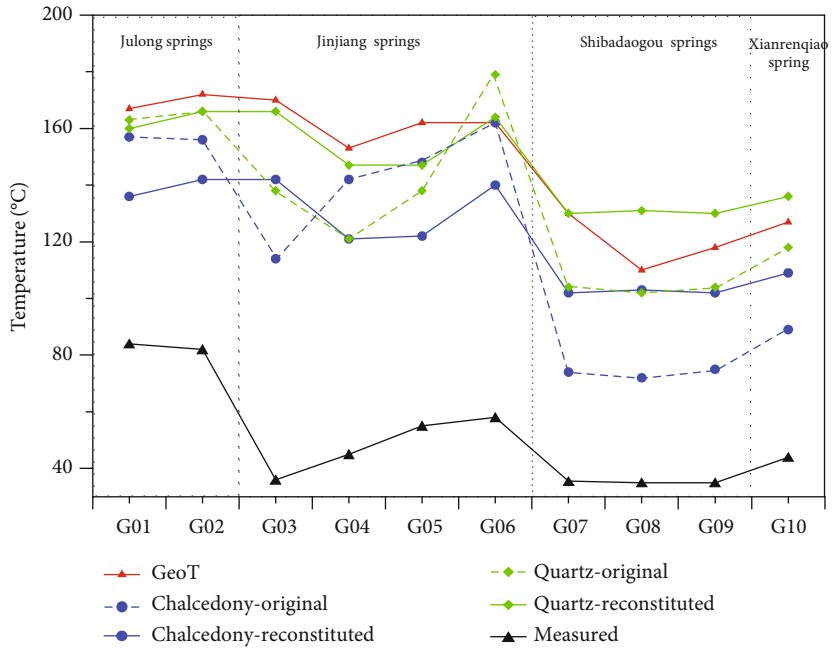

Figure 6: Comparison of temperatures obtained from the integrated multicomponent geothermometry method with those calculated by classic geothermometers.

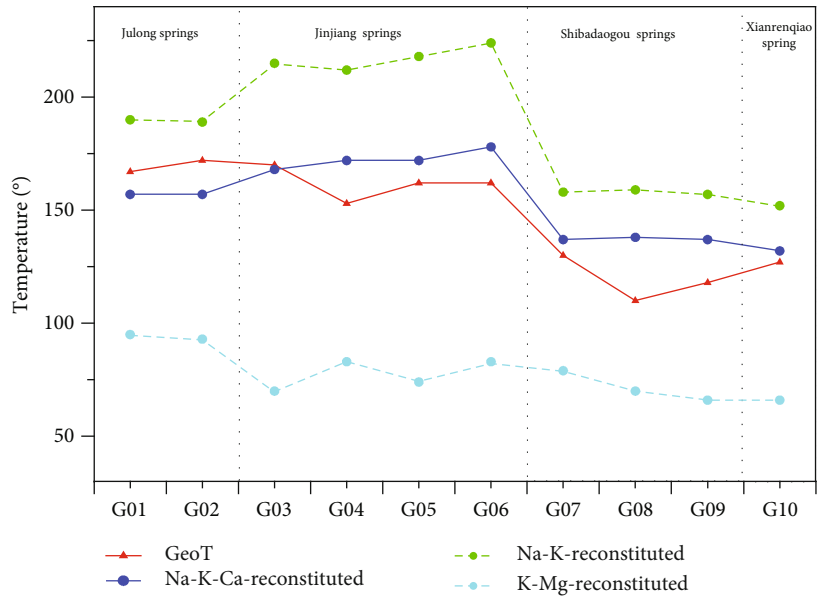

Figure 7: Difference in temperature estimates for the reconstituted deep fluid using classic geothermometers.

reservoir depth and geothermal circulation depth can be estimated using the following equations:

$$h = \frac{t_1 - t_2}{\Delta t}, \quad (1)$$

$$H = G(t_1 - t_0) + H_0, \quad (2)$$

where h is the reservoir depth (km), t_1 is the geothermal reservoir temperature (°C), t_2 is the recharge source temperature (°C), Δt is the geothermal gradient (°C/100 m) [12], H is the geothermal circulation depth (km), G is the reciprocal of the geothermal degree, t_0 is the average temperature (°C), and H_0 is the geothermal atmospheric temperature zone depth (m).

The reservoir depth and geothermal circulation depth of different thermal springs in the Changbai Mountain volcanic region are listed in Table 3. The reservoir depth and geothermal circulation of the Julong thermal springs are 4.76~4.91 km and 4.82~4.97 km, respectively. The reservoir

Table 3: Geothermal deep circulation characteristics of different thermal springs in the Changbai Mountain region.

Thermal springs	Sample no.	t_0 (°C)	t_1 (°C)	t_2 (°C)	Δt (°C/100 m)	G	H_0 (m)	h (km)	H (km)
Julong springs	G01	4	167	5	3.4	29.41	30	4.76	4.82
	G02	4	172	5	3.4	29.41	30	4.91	4.97
Jinjiang springs	G03	4	170	5	3.4	29.41	30	4.85	4.91
	G04	4	153	5	3.4	29.41	30	4.35	4.41
	G05	4	162	5	3.4	29.41	30	4.62	4.68
	G06	4	162	5	3.4	29.41	30	4.62	4.68
Shibadaogou springs	G07	4	130	5	2.8	35.71	30	4.46	4.53
	G08	4	110	5	2.8	35.71	30	3.75	3.82
	G09	4	118	5	2.8	35.71	30	4.36	4.42
Xianrenqiao springs	G010	4	127	5	3.0	33.33	30	4.07	4.13

depth and geothermal circulation of the Jinjiang thermal springs are 4.35~4.85 km and 4.41~4.91 km, respectively. The reservoir depth and geothermal circulation of the Shibadaogou thermal springs are 3.75~4.46 km and 3.82~4.53 km, respectively. The reservoir depth and geothermal circulation of the Xianrenqiao thermal springs are 4.07 and 4.13 km, respectively. The reservoir and geothermal circulation depths of the Julong and Jinjiang springs are even deeper than those of the Shibadaogou and Xianrenqiao springs, and their water chemistry may reflect more deep geochemical information in the Changbai Mountain region.

6. Conclusions

Based on the IMG method using GeoT, we investigated geothermal reservoir temperatures for the four major thermal springs in the Changbai Mountain volcanic region, China. The following conclusions can be drawn on the basis of this study:

(1) In addition to the use of the Fix-Al-HCO_3^- method, the numerical optimizations of the dilution factor and steam fraction are applied to reconstruct the original deep water compositions and then estimate the reservoir temperatures. Compared with the classic geothermometers, this approach can quantify processes affecting the fluid chemical composition in spring genesis and yield reasonable temperatures

(2) The geothermal reservoir temperatures of the four major thermal springs range from 110 to 172°C by IMG. Moreover, the reservoir temperatures for the Julong and Jinjiang thermal springs range from 153 to 172°C and are significantly greater than those for the Shibadaogou and Xianrenqiao thermal springs (110~130°C)

(3) The reservoir depths and geothermal circulation depths for these thermal springs are 3.75~4.91 km and 3.82~4.97 km, respectively. Compared to the Shibadaogou and Xianrenqiao springs, the water chemistry for the Julong and Jinjiang thermal springs may reflect deeper geofluid information in the Changbai Mountain region

(4) The thermal springs in the Changbai Mountain volcanic region is favored for the exploitation of the geothermal water. Considering reservoir temperature, power generation development of geothermal utilization in the Julong and Jinjiang geothermal field should be evaluated

Data Availability

The measured data used to support the findings of this study are included within the article.

Conflicts of Interest

The authors declare that they have no conflicts of interest.

Acknowledgments

This work was supported by the National Key R&D Program of China (2016YFC0402803-02), National Natural Science Foundation of China (Grant Nos. 41807194, 41902263 and 41807208), Major Scientific and Technological Projects of Jilin Province (0773-1441GNJL00390), Scientific Research Initiation Funds for PhD Scholars (BQ2017011), China's Post-doctoral Science Fund (2018M631874), Scientific Research Projects of the Higher University in Hebei (ZD2019082), Hebei Province Water Conservancy Science and Technology Plan Projects (2017-59), Youth Foundation of Hebei Province Department (QN2017026), Natural Science Fund Project in Hebei Province (D2018403040), Hebei Key Laboratory of Geological Resources and Environmental Monitoring and Protection Fund (JCYKT201901), Natural Science Foundation of Hubei Province of China (2018CFB258), State Key Laboratory of Groundwater Protection and Utilization of Coal Mining (SHJT-17-42.9), the Engineering Research Center of Geothermal Resources Development Technology and Equipment, Ministry of Education, Jilin University, and Scientific Research Foundation of Yangtze University (802100270303).

References

[1] R. Fournier, "A revised equation for the Na/K geothermometer," *Geothermal Resources Council Transactions*, vol. 3, pp. 221–224, 1979.

[2] W. F. Giggenbach, "Geothermal solute equilibria. Derivation of Na-K-Mg-Ca geoindicators," *Geochimica et Cosmochimica Acta*, vol. 52, no. 12, pp. 2749–2765, 1988.

[3] R. O. Fournier and A. H. Truesdell, "An empirical Na-K-Ca geothermometer for natural waters," *Geochimica et Cosmochimica Acta*, vol. 37, no. 5, pp. 1255–1275, 1973.

[4] R. O. Fournier and R. W. Potter, "Revised and expanded silica (quartz) geothermometer," *Bulletin Geothermal Resources Council*, vol. 11, pp. 3–12, 1982.

[5] B. Yan, S. W. Qiu, Z. Liu, and X. Changlai, "Characteristics of the geothermal water in Changbai Mountain volcanic region, northeast of China," *Arabian Journal of Geosciences*, vol. 10, no. 12, p. 261, 2017.

[6] M. Reed and N. Spycher, "Calculation of pH and mineral equilibria in hydrothermal waters with application to geothermometry and studies of boiling and dilution," *Geochimica et Cosmochimica Acta*, vol. 48, no. 7, pp. 1479–1492, 1984.

[7] L. Peiffer, C. Wanner, N. Spycher, E. L. Sonnenthal, B. M. Kennedy, and J. Iovenitti, "Optimized multicomponent vs. classical geothermometry: insights from modeling studies at the Dixie Valley geothermal area," *Geothermics*, vol. 51, pp. 154–169, 2014.

[8] T. Xu, Z. Hou, X. Jia et al., "Classical and integrated multicomponent geothermometry at the Tengchong geothermal field, Southwestern China," *Environmental Earth Sciences*, vol. 75, no. 24, p. 1502, 2016.

[9] F. Tian and D. P. Tang, "Petrogenesis of the Cenozoic volcanic rocks in the Changbaishan region," *Acta Petrologica Sinica*, vol. 5, no. 2, pp. 49–64, 1989.

[10] H. Wei, Y. Wang, J. Jin, L. Gao, S. H. Yun, and B. Jin, "Timescale and evolution of the intracontinental Tianchi volcanic shield and ignimbrite-forming eruption, Changbaishan, Northeast China," *Lithos*, vol. 96, no. 1-2, pp. 315–324, 2007.

[11] P. Chen, *The Formation Conditions and Main Controlling Factors of Geothermal Resources in Songjianghe Area of Changbai Mountain*, Jilin University, 2018.

[12] B. Yan, "Study on the formation mechanism of geothermal water resources in Changbai Mountain basalt area," *Jilin University*, pp. 88–126, 2016.

[13] B. Yan, X. Liang, and C. Xiao, "Hydrogeochemical characteristics and genesis model of Jinjiang and Julong hot springs in Changbai Mountain, Northeast China," *Geofluids*, vol. 2018, Article ID 1694567, 16 pages, 2018.

[14] A. Zaporozec, "Graphical interpretation of water-quality data," *Ground Water*, vol. 10, no. 2, pp. 32–43, 1972.

[15] N. Spycher, L. N. Peiffer, and E. Sonnenthal, *GeoT User's Guide: A Computer Program for Multicomponent Geothermometry and Geochemical Speciation, Version 1.4*, Lawrence Berkeley National Laboratory, 2014.

[16] N. Spycher, E. Sonnenthal, and B. Kennedy, "Integrating multicomponent chemical geothermometry with parameter estimation computations for geothermal exploration," *GRC Transactions*, vol. 35, pp. 663–666, 2011.

[17] N. Spycher, S. Finsterle, and P. Dobson, "New developments in multicomponent geothermometry," in *Proceedings of 41st Workshop on Geothermal Reservoir Engineering*, Stanford University, Stanford, California, February 2016.

[18] T. Xu and K. Pruess, "On fluid flow and mineral alteration in fractured caprock of magmatic hydrothermal systems," *Journal of Geophysical Research: Solid Earth*, vol. 106, no. B2, pp. 2121–2138, 2001.

[19] T. Xu, E. Sonnenthal, N. Spycher, and K. Pruess, "TOUGHREACT–A simulation program for non-isothermal multiphase reactive geochemical transport in variably saturated geologic media: Applications to geothermal injectivity and CO_2 geological sequestration," *Computers & Geosciences*, vol. 32, no. 2, pp. 145–165, 2006.

[20] T. Xu, N. Spycher, E. Sonnenthal, G. Zhang, L. Zheng, and K. Pruess, "TOUGHREACT version 2.0: a simulator for subsurface reactive transport under non-isothermal multiphase flow conditions," *Computers & Geosciences*, vol. 37, no. 6, pp. 763–774, 2011.

[21] M. Reed, "Calculation of simultaneous chemical equilibria in aqueous-mineral-gas systems and its application to modeling hydrothermal processes," in *Techniques in Hydrothermal Ore Deposits Geology*, vol. 10, pp. 109–124, 1998.

[22] M. H. Reed, "Calculation of multicomponent chemical equilibria and reaction processes in systems involving minerals, gases and an aqueous phase," *Geochimica et Cosmochimica Acta*, vol. 46, no. 4, pp. 513–528, 1982.

[23] R. O. Fournier, "Chemical geothermometers and mixing models for geothermal systems," *Geothermics*, vol. 5, no. 1-4, pp. 41–50, 1977.

[24] F. Gherardi and N. Spycher, "Application of integrated multicomponent geothermometry at the Chachimbiro thermal area, a difficult geothermal prospection case," https://earth.stanford.edu.

[25] N. Spycher, L. Peiffer, E. L. Sonnenthal, G. Saldi, M. H. Reed, and B. M. Kennedy, "Integrated multicomponent solute geothermometry," *Geothermics*, vol. 51, pp. 113–123, 2014.

[26] C. Wanner, L. Peiffer, E. Sonnenthal, N. Spycher, J. Iovenitti, and B. M. Kennedy, "Reactive transport modeling of the Dixie Valley geothermal area: insights on flow and geothermometry," *Geothermics*, vol. 51, pp. 130–141, 2014.

[27] Z.-H. Pang and M. Reed, "Theoretical chemical thermometry on geothermal waters: problems and methods," *Geochimica et Cosmochimica Acta*, vol. 62, no. 6, pp. 1083–1091, 1998.

[28] J. L. Palandri and M. H. Reed, "Reconstruction of in situ composition of sedimentary formation waters," *Geochimica et Cosmochimica Acta*, vol. 65, no. 11, pp. 1741–1767, 2001.

[29] M. Reed and J. Palandri, "SOLTHERM. H06, a database of equilibrium constants for minerals and aqueous species," University of Oregon, Eugene, Oregon, 2006.

[30] Y. Wang, "A preliminary study on developed mechanism of karst in carbonate rock region, Zhenzhumen formation, Laoling group, in the southern part of Jilin province," *Jilin Geology*, vol. 1992, no. 03, 28 pages, 1992.

[31] N. Lian, "Geological features of dolomite marble deposit in Dongchang District Jinchang Town of Tonghua City," *Jilin Province*, vol. 36, no. 2, pp. 34–38, 2017.